Virology Journal

RESEARCH

Open Access

Identification and characterization of a novel reovirus strain isolated fromgrass carp (*Ctenopharyngodon idella*)

Weiguang Kong[1], Guangyi Ding[1], Qiushi Zhang[1], Xinjie Yuan[1], Yuchao Zhu[1], Liyuan Ma[1], Chang Cai[1], Yong Shi[1], Qianqian Zhang[1] and Zhen Xu[1*]

Abstract

Background Grass carp (*Ctenopharyngodon idella*) hemorrhagic disease (GCHD) is a devastating disease that leads to substantial economic losses in the freshwater aquaculture industry.

Results In this study, we investigated an outbreak of GCHD in large-scale grass carp and identified GCRV-II infection. Notably, hematoxylin and eosin (H&E) staining showed severe histopathological changes in the spleen, head kidney, gill, and gut. Furthermore, we sequenced the entire genome of the viral isolate, and multiple sequence alignment and phylogenetic tree analysis indicated that it represents a novel strain of GCRV-II, provisionally named GCRV-YX246. Finally, artificial infection experiments confirmed the strong virulence, high mortality, and severe pathological damage caused by GCRV-YX246, as demonstrated through artificial infection.

Conclusions A novel reovirus from large-scale grass carp cultured in China was identified. The discovery of this novel GCRV-II strain enhances our understanding of GCRV-II biology and provides valuable insights for developing more effective prevention strategies for GCHD.

Keywords Grass carp reovirus, Identification, Genome, Pathogenicity, Phylogenetic analysis

Background

Grass carp hemorrhagic disease (GCHD) is a highly contagious and fatal viral disease caused by the Grass Carp Reovirus (GCRV), resulting in substantial economic losses for the aquaculture industry [1]. The Ministry of Agriculture and Rural Affairs of China has classified GCHD as a Class II animal disease [2]. GCRV infects a variety of hosts, including black carp (*Mylopharyngodon piceus*) [3], grass carp (*Ctenopharyngodon idella*) [4], silver carp (*Hypophthalmichthys molitrix*) [5], bighead carp (*Aristichthys nobilis*) [6], crucian carp (*Carassius carassius*) [7], common carp (*Cyprinus carpio*) [8], and rare minnow (*Gobiocypris rarus*) [9]. GCHD commonly affects juvenile and yearling grass carp during breeding, leading to severe clinical symptoms of bleeding and high mortality rates [10]. In recent years, the disease has expanded its impact from seedlings to large grass carp, although information on the isolation of related viral strains remains limited.

GCRV belongs to the genus *Aquareovirus* within the family *Reoviridae* [11]. The virus particle is a non-enveloped, icosahedral particle encased in multiple concentric protein capsid, with its genome composed of 11 double-stranded RNA (dsRNA) segments [12]. The segmented

*Correspondence:
Zhen Xu
zhenxu@ihb.ac.cn
[1]State Key Laboratory of Breeding Biotechnology and Sustainable Aquaculture, Institute of Hydrobiology, Chinese Academy of Sciences, Wuhan 430072, China

nature of the genome contributes to the high complexity and variability observed among different GCRV strains [13]. Generally, GCRV isolates are categorized into three genotypes (I, II, and III), with representative strains including GCRV-873 (Genotype I), GCRV-HZ08 (Genotype II), and GCRV-104 (Genotype III) [14]. These isolates differ significantly in virulence, cell culture properties, immunogenicity, and pathogenicity. Genotypes I and III isolates, such as GCRV-873, GCRV-096, and GCRV-JX01, are considered low-virulence strains and rarely cause clinical symptoms. In contrast, Genotype II, which includes strains GCRV-HZ08, GCRV-109, GCRV-JX02, and GCRV-AH528, is currently the predominant epidemic genotype [15]. Infections with GCRV-II result in extensive virion proliferation, tissue necrosis, and severe punctate hemorrhages in the muscle, fins, oral cavity, and internal organs [16]. However, virulence varies among GCRV-II isolates. For example, grass carp infected with the HZ08 strain exhibited mild clinical symptoms and a mortality rate of around 75% [17], whereas the HuNan1307 and GD108 strains caused severe bleeding symptoms and mortality rates reaching up to 100% [14]. This phenotypic variability highlights the importance of further exploring the biological, sequence, and virulence characteristics of highly virulent GCRV strains.

The isolation and identification of viruses are crucial for the prevention and treatment of viral diseases [18]. As viruses are obligatory intracellular parasites necessitating living cells for replication, cultured cells, eggs, and laboratory animals are commonly employed for virus isolation [19]. Currently, there are no cell lines highly sensitive to GCRV-II, and GCRV-II-infected cells do not exhibit significant cytopathic effects (CPE) [16]. Notably, when GCRV-II is isolated using existing cell lines, reinfection in grass carp often fails to produce noticeable clinical symptoms or high mortality [20].

In this study, a novel reovirus strain, tentatively named GCRV-YX246, was isolated from diseased grass carp in Hubei Province, China, in 2024. The clinical symptoms of natural GCRV-II infection were investigated in detail. Additionally, the entire genome of GCRV-YX246 was cloned, sequenced, and analyzed, revealing distinct molecular characteristics compared to other aquareoviruses (AQRVs) and orthoreoviruses (ORVs). Importantly, we examined the infectivity of GCRV-YX246 under different infection modes through artificial infection experiments. The isolation of GCRV-YX246 holds significant scientific and practical value for establishing infection models, studying pathogenic mechanisms, and developing vaccines.

Materials and methods

Naturally diseased fish and sample collection

The diseased grass carp (approximately 13 months old), with an average body length of 29.3 ± 5.4 cm and an average weight of 216.3 ± 13.6 g) were obtained from a farm in Yangxin County, Huangshi City, Hubei Province. Tissues such as the head kidney (HK), spleen (SP), muscle, brain, skin, liver, mouth, gill, and gut were collected for GCRV-II detection. The remaining fish were stored at − 80 ℃ for virus identification and isolation.

Histology, light microscopy, and Immunofluorescence

The SP, HK, gill, and gut of the grass carp were fixed overnight in 4% neutral buffered formalin. Following fixation, the tissues were dehydrated with an ethanol gradient, embedded in paraffin, and sectioned to a thickness of 5 μm. Sections were stained with hematoxylin and eosin (H&E), and an optical microscope was used to examine the pathological changes. For GCRV detection, sections were incubated with 2 μg/mL mouse anti-GCRV-*VP4* polyclonal antibody at 4 ℃ overnight, followed by incubation with 2 μg/mL Cy3-conjugated goat anti-mouse IgG for 30 min. Prior to fixation, the nuclei were stained with DAPI (Invitrogen, USA) for 8 min. All sections were observed under an Olympus BX53 microscope (Olympus, Japan) and images were captured using the CellSense Dimension software (Olympus, Japan).

RNA extraction, cDNA preparation, and virus detection

Total RNA from diseased, healthy and infected grass carp was extracted using TRIZOL Reagent (Qinke, China), and the RNA quantity and concentration were measured using a spectrophotometer (Nanodrop ND2000, Thermo Fisher Scientific, USA). cDNA synthesis was performed using the Hifair® II 1st Strand cDNA Synthesis Kit with 1 μg of total RNA, and the resulting cDNA was used directly for subsequent PCR or qPCR reactions. Nested PCR was employed to detect GCRV-II RNA in various tissues for GCRV identification. In addition, GCRV-II viral copies were quantified using absolute quantitative polymerase chain reaction (qPCR) with GCRV-II-S7 specific primers and TaqMan probes [21]. The qPCR program consisted of a first step at 95 ℃ for 5 min, followed by 40 cycles at 95 ℃ for 10 s, and 58 ℃ for 30 s. All samples were run in duplicate. Standard curves were generated by performing serial dilutions of plasmids with known copy numbers of the GCRV-II-S7 gene. The viral load was calculated by extrapolating the mean of each gene copy number from the standard curve. The primers used for nested PCR and absolute qPCR are shown in Table S1.

Transmission electron microscopy

To examine the morphology of virus particles in tissues from grass carp naturally infected with GCRV-II, all clinical tissue samples were fixed overnight in electron microscopy fixative and rinsed with 0.1 M phosphate buffer (pH 7.4). The fixed tissues were then transferred to 1% OsO_4 in 0.1 M phosphate buffer for 2 h and rinsed three times with 0.1 M phosphate buffer. The tissues were dehydrated through a graded series of ethanol and acetone, and finally embedded in molds for polymerization at 60 ℃ for 48 h. Ultrathin sections of the resin blocks were transferred onto copper grids and stained with 2% uranyl acetate and 2.6% lead citrate before being examined by TEM (HT-7700, Tokyo, Japan). Images were captured at the Institute of Hydrobiology, Chinese Academy of Sciences.

Viral metagenomics sequencing, 5′ and 3′ end sequencing

Total RNA was extracted from tissues with high viral loads using TRIzol reagent, and samples were sent to Auqo Dingsheng Biotech (Wuhan, China) for viral metagenomic sequencing. Sequencing was conducted on the Illumina NovaSeq 6000 platform, generating reads with an average length of 150 bp. High-quality reads were then assembled into contigs using the *de novo* assembler SPAdes version 3.13.1. However, viral metagenomics sequencing alone was insufficient to obtain the entire GCRV-YX246 genome without pre-amplification. Only the coding DNA sequences (CDS) of the S1–S11 fragments were retrieved through metagenomics sequencing. Therefore, we designed primers (listed in Table S1) to amplify the entire GCRV-YX246 genome using the SMARTer RACE 5′/3′ Kit (Clontech, Mountain View, CA, USA). The PCR amplification program was performed under the following conditions: initial denaturation at 98 ℃ for 3 min, followed by 30 cycles at 98 ℃ for 10 s, 68 ℃ for 20 s and 72 ℃ for 30 s and a final extension at 72 ℃ for 5 min. PCR products were then purified using a gel extraction kit (Takara, Winooski, VT, USA) according to the manufacturer's instructions and cloned into a pCE3-Blunt Cloning vector (Vazyme, Nanjing, China). The ligation products were transfected into DH5α competent cells, and positive recombinant plasmids were sequenced using M13 forward and M13 reverse primers. The whole-genome sequence was assembled using the splicing method in the SEQMAN software.

Viral genome sequence bioinformatic analysis

The sequences of Aquareovirus and other reovirus strains employed for comparison in this study were sourced from GenBank. BLAST searches were conducted to locate related nucleic acid and protein entries within the National Center for Biotechnology Information (NCBI) database. The genomic DNA sequences and deduced amino acid sequences of GCRV-YX246 were analyzed using EditSeq (DNASTAR 5.0) and BioXM software (http://202.195.246.60/BioXM/). Genomic circos plots were generated using Genovi software, and evolutionary coefficients (πN/πS) were calculated with HYPHY software. Multiple sequence alignments were performed using the ClustalW program, and phylogenetic analyses were conducted with Molecular Evolutionary Genetics Analysis version 7.0 (MEGA7.0). Phylogenetic trees were constructed using the neighbor-joining method based on RNA-dependent RNA polymerase (RdRp) and VP6 sequences, with 1,000 bootstrap replications performed in the MEGA program.

Artificial infection

To assess the pathogenicity of GCRV-YX246, infection models were established in grass carp (approximately 4 months old), with an average body length of 9.5 ± 0.74 cm and an average weight of 10.3 ± 1.77 g) and rare minnows (approximately 12 months old), with an average body length of 4.9 ± 0.54 cm and an average weight of 1.3 ± 0.36 g). grass carp and rare minnows were each orally infused with 100 μL of virus-containing tissue homogenate or virus-free tissue homogenate. Mortality was observed daily, and dead fish were sampled throughout the experimental period. Tissues, including the HK, SP, gill, and gut, were collected to assess viral load and pathological changes at 7 days post-infection (dpi).

Results

A unique GCRV-II infection event occurred in large-scale grass carp

A suspected outbreak of GCHD was identified, and a series of laboratory tests were conducted to investigate the cause. Clinical examination revealed pronounced hemorrhages around the eyes, gill covers, oral cavity, and the bases of the fins. A further autopsy revealed typical severe hemorrhaging in the muscle, a red, swollen, and congested gut, and an enlarged SP (Fig. 1A). Based on the timing of disease onset and these initial observations, GCHD was suspected. RNA samples from nine tissues, including muscle, brain, skin, and intestine, were analyzed via nested PCR targeting the GCRV-II RNA-dependent RNA polymerase (RdRp) gene, which confirmed GCRV-II infection (Fig. 1B). Furthermore, absolute quantification of viral mRNA in different tissues indicated that the muscle and brain tissues had the highest viral loads, while the liver had the lowest (Fig. 1C). Immunofluorescence microscopy further demonstrated GCRV-II infection at the protein level (Fig. 1D). TEM analyses also revealed virus particles in the SP, HK, gill, and gut tissues of the diseased fish, showing particles with a spherical shape, two capsid layers (Fig. 1E).

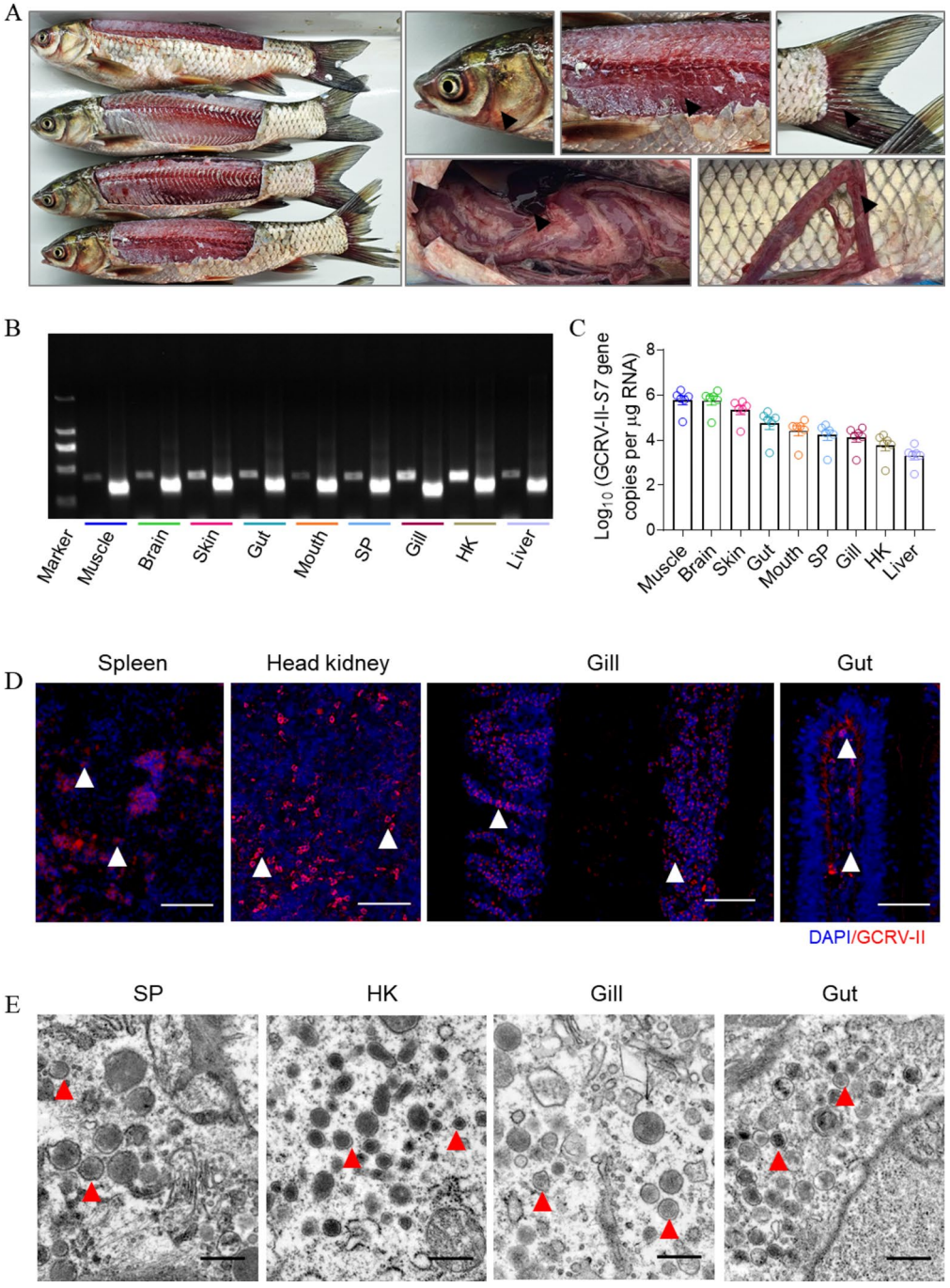

Fig. 1 Pathogenic characteristics and identification of GCRV-YX246. **A** Clinical symptoms observed in diseased grass carp (*Ctenopharyngodon idellus*). **B** Nested PCR products showing bands at 408 bp and 363 bp from GCRV cDNA. **C** Viral loads detected in different tissues of diseased grass carp ($n=6$). Muscle and brain exhibited the highest viral loads, followed by skin and gut. **D** Immunofluorescence analysis of the SP, HK, gut, and gills under natural infection conditions. The white arrows indicate the presence of GCRV-II virus. Scale bar, 50 μm. **E** TEM images of the SP, HK, gut, and gills under natural infection conditions. The red arrows point to GCRV-II virions. Scale bar, 500 nm

Histological examination

Histopathological analysis of SP, HK, gill, and gut tissues from diseased fish was performed using H&E staining. In the SP, cytoplasmic vacuolization, congestion, focal necrosis, and tissue laxity were observed (Fig. 2A). The HK showed damage to the renal tubular epithelial cells, gaps between the tubules and surrounding tissues, and congestion of the renal interstitium (Fig. 2B). In the gill tissue, pathological alterations were seen in both primary and secondary lamellae, including hemorrhaging and fusion. Additionally, the gill epithelial cells were severely separated from the capillaries, and the chondrocytes in

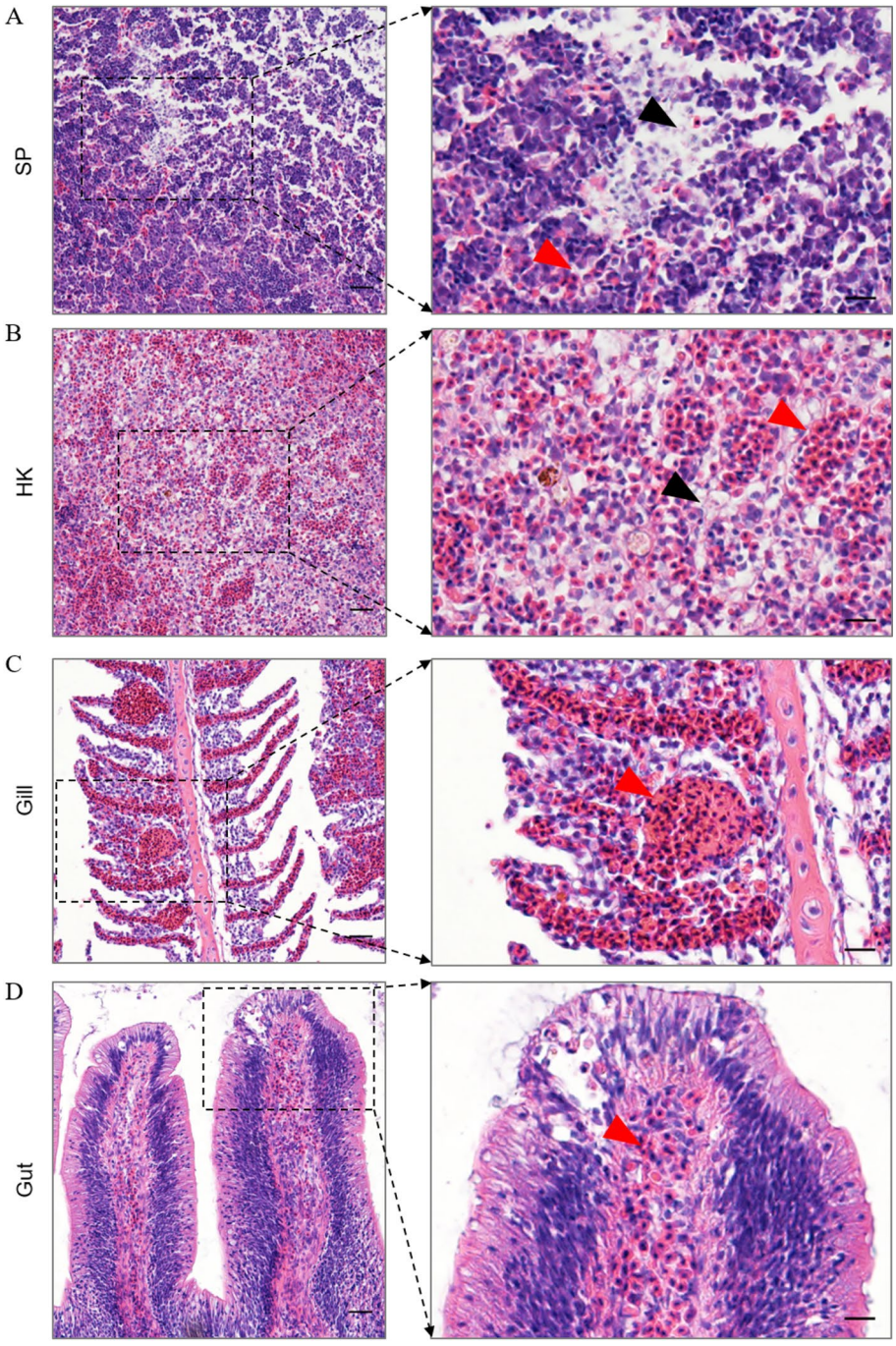

Fig. 2 Histopathological changes in the SP, HK, gill, and gut of fish naturally infected with GCRV-II. Histological examination of the SP (**A**), HK (**B**), gill (**C**), and gut (**D**) from naturally infected fish. Red arrows indicate erythrocyte infiltration, while black arrows mark areas of cellular necrosis. Scale bar, 50 μm

the gill filaments were disorganized (Fig. 2C). In the gut tissue, broken gut villi, dilated capillaries, and congestion in the lamina propria were evident (Fig. 2D). These findings confirm that GCRV-II infection in grass carp resulted in severe pathological damage across multiple tissues.

Cloning of GCRV- YX246

The genome of GCRV-YX246 was sequenced using the Illumina Novaseq platform, with assembly performed using SPAdes software v3.0.1. The total genomic length of GCRV-YX246 was determined to be 24,751 bp, which is consistent with the genomic lengths of other viruses in the *Reoviridae* family, ranging between 18,500 and 29,210 bp (S1-S11 GenBank accession number:

PQ553626–PQ553636). The G + C content of GCRV-YX246 was 49.95%, which is lower than that of aquareoviruses (52–60%) but higher than that of orthoreoviruses (44–48%) (Fig. 3). The GCRV-YX246 genome consists of 11 segments, labeled S1–S11 based on sequence length. These segments range from 3.9 kb to 1 kb, with each encoding a single protein. All segments exhibited conserved terminal nucleotide sequences, with GUAAU/CU at the 5' end and A/UUCAUC at the 3' end (Table 1).

Sequence analysis of GCRV-YX246

Based on predictive analyses, the S1 segment of the GCRV-YX246 genome encodes the core protein VP1, consisting of 1,294 amino acids (AA). BLASTp searches showed that VP1 contains conserved domains related to the reovirus L2 superfamily, including sequences from the lambda-2 (L2) core spike protein of reovirus, indicating that VP1 may act as an mRNA capping enzyme. VP1 of GCRV-YX246 shares 29.72–99.38% sequence identity with VP1 homologs from related aquareoviruses. The S2 segment encodes the core protein VP2 (1,272 AA), which serves as the RNA-dependent RNA polymerase (RdRp). GCRV-YX246 VP2 shares 45.82–99.84% identity with its homologs in related aquareoviruses. The S3 segment encodes the core protein VP3 (1,214 AA), serving as an NTPase and helicase, in line with previous research findings. GCRV-YX246 VP3 shares 36.80–99.59% identity with homologs from other aquareoviruses. The S4 segment encodes the nonstructural protein NS79 (717 AA), which is smaller than the corresponding proteins found

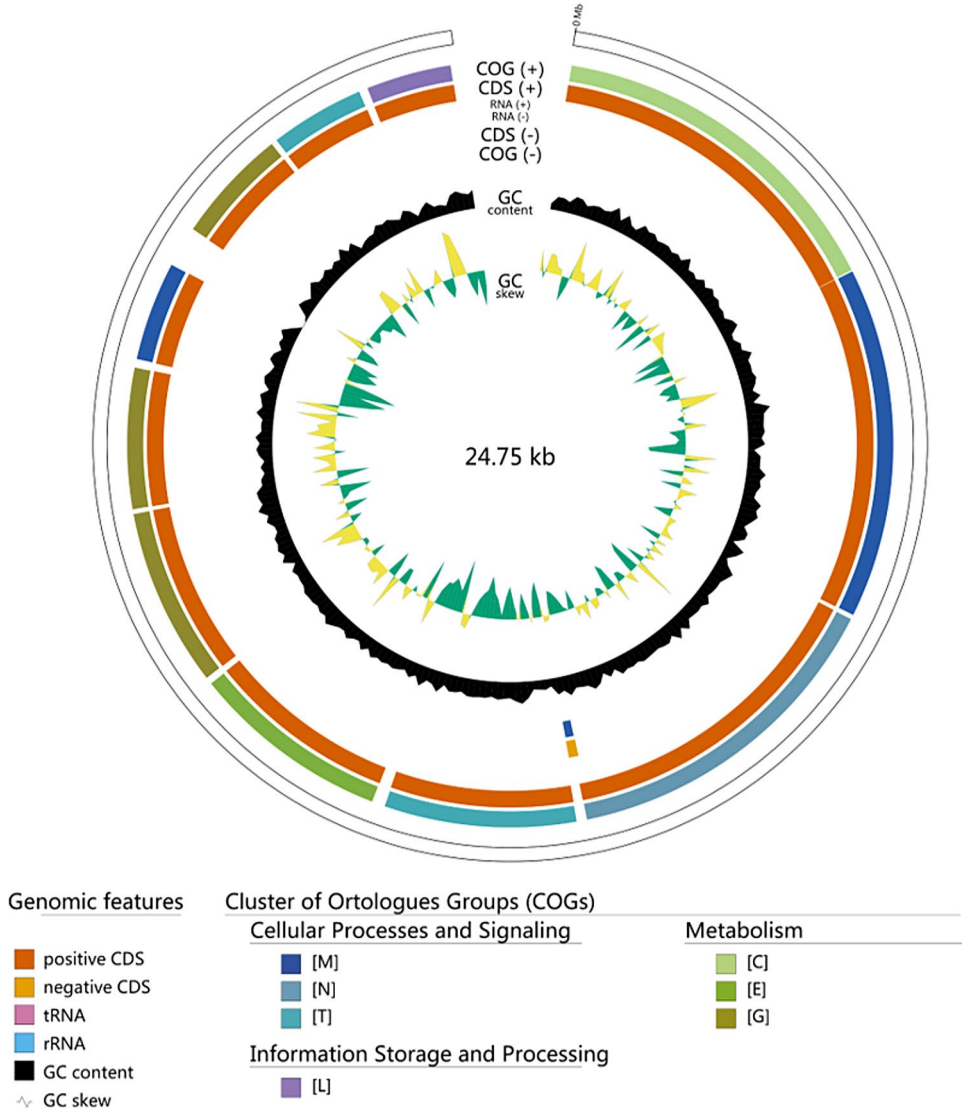

Fig. 3 Circular map of the GCRV-YX246 genome. Each circular map represents a replicon from the complete genome. GCRV-YX246 genome consists of 11 segments RNA strand (scale variable). Labeling from outside to the inside: Contigs; COGs on the forward strand; CDS, tRNAs, and rRNAs on the forward strand; CDS, tRNAs, and rRNAs on the reverse strand; COGs on the reverse strand; GC content; GC skew

Table 1 Characterization of GCRV-YX246 genomic fragments, predicted protein functions and conserved terminal sequences

Segment/nt	Length (bp)	GC%	Average coverage (x)	5'NCR	3'NCR	CDS	Protein (aa)	MM (kDa)	Predicted Function	Conserved Terminal Sequences
S1	3928	49.77	54.4	17	26	18-3902	VP1/1294	143.72	Core protein guanylyltransferase	5'-GUAAUU UUCAUC-3'
S2	3867	50.30	71.4	12	36	13-3831	VP2/1272	142.46	Core protein polymerase	5'-GUAAUU AUCAUC-3'
S3	3753	50.63	55.8	15	39	16-3714	VP3/1232	135.77	Core protein NTPase, helicase	5'-GUAAUU UUCAUC-3'
S4	2310	51.43	89.8	24	132	25-2178	NS79/717	79.27	Nonstructural protein	5'-GUAUUU UUCAUC-3'
S5	2230	49.82	91.4	12	37	13-2193	VP5/726	80.66	Core protein NTPase	5'-GUAACU UUCAUC-3'
S6	2028	50.89	109.5	40	35	41-1993	VP4/650	68.33	Outer capsid	5'-GUAAUU UUCAUC-3'
S7	1604	48.75	130.8	17	48	18-1556	VP56/512	55.96	Fiber protein	5'-GUAAUU UUCAUC-3'
S8	1560	46.09	224.6	47	427	48-1133	VP41/361	41.27	Core protein	5'-GUAAUU UGCAUC-3'
S9	1320	50.08	104	22	41	23-1279	VP6/418	47.99	Core protein	5'-GUAACU UUCAUC-3'
S10	1124	49.73	671.7	24	62	25-1062	NS38/345	38.43	Nonstructural protein	5'GUAAUU UUCAUC-3'
S11	1027	49.85	297.1	34	60	35–967	VP35/310	35.50	Outer clamp protein	5'-GUAAUU UUCAUC-3'

in other aquareovirus species. NS79 of GCRV-YX246 shares 23.23–99.02% sequence identity with the NS1 protein of related aquareoviruses. The S5 segment encodes the core protein VP5 (726 AA), with 23.56–99.59% identity to homologs in related aquareoviruses. Based on BLASTp analysis, we found VP5 contains conserved domains associated with the reovirus Mu-2 superfamily, suggesting that VP5 may play a critical role in the formation and structural organization of viral inclusion bodies. The S6 segment encodes the outer capsid protein VP4 (650 AA), sharing 27.11–99.23% identity with VP4 homologs from other aquareoviruses. Notably, VP4 contains conserved domains associated with the reovirus M2 superfamily, indicating that VP4 may play a role in the penetration of host cell membranes. The S7 segment encodes the outer capsid protein VP56 (512 AA), with GCRV-YX246 sharing 22.19–98.44% identity with its homologs in other aquareoviruses. BLASTp searches revealed that VP56 contains sequences belonging to the adenovirus fiber protein, suggesting that VP56 may play a key role in viral entry into the nucleus. The S8 genome segment encodes the core protein VP41 (361 AA). None homologous protein of VP41 were found in already classified aquareoviruses. The S9 segment encodes the nonstructural protein VP6 (418 AA), with VP6 sharing 22.62–99.80% identity with its homologs from related aquareoviruses. The S10 segment encodes the nonstructural protein NS38 (345 AA). No protein homologs of NS38 were identified in previously classified aquareoviruses. The S11 genome segment encodes the outer capsid protein VP35 (310 AA). Since the zinc-binding motif of exocystin, CxxC-n16-HxC, can be found at amino acids 50–73 of the protein, VP35 was identified as a putative outer capsid protein.

In summary, GCRV-YX246 encodes 11 proteins and closely resembles other GCRV strains. Based on comparative analysis, it was observed that the genome segments and their encoded proteins in GCRV-YX246, GCRV-HZ08, GCRV-873, and GCRV104 exhibit significant similarity, with GCRV-HZ08 emerging as the most closely related strain (Fig. 4). The nucleotide and amino acid sequence identities between GCRV-YX246 and other GCRV strains are summarized in Table 2, with the GCRV-II strains showing the highest levels of amino acid sequence identities.

Phylogenetic analysis

To assess the phylogenetic relationships between GCRV-YX246 and other *Reoviridae* isolates, a phylogenetic tree based on the amino acid sequence of the highly conserved RNA polymerase was constructed using MEGA software. The analysis showed that all known species of *Aquareovirus* formed a distinct clade. Within this clade, GCRV-YX246 was most closely related to GCRV-DY197, followed by other *Reoviridae* isolates (Fig. 5).

Additionally, to further investigate the phylogenetic relationships between GCRV-YX246 and other *Aquareovirus* isolates, a phylogenetic tree based on the amino

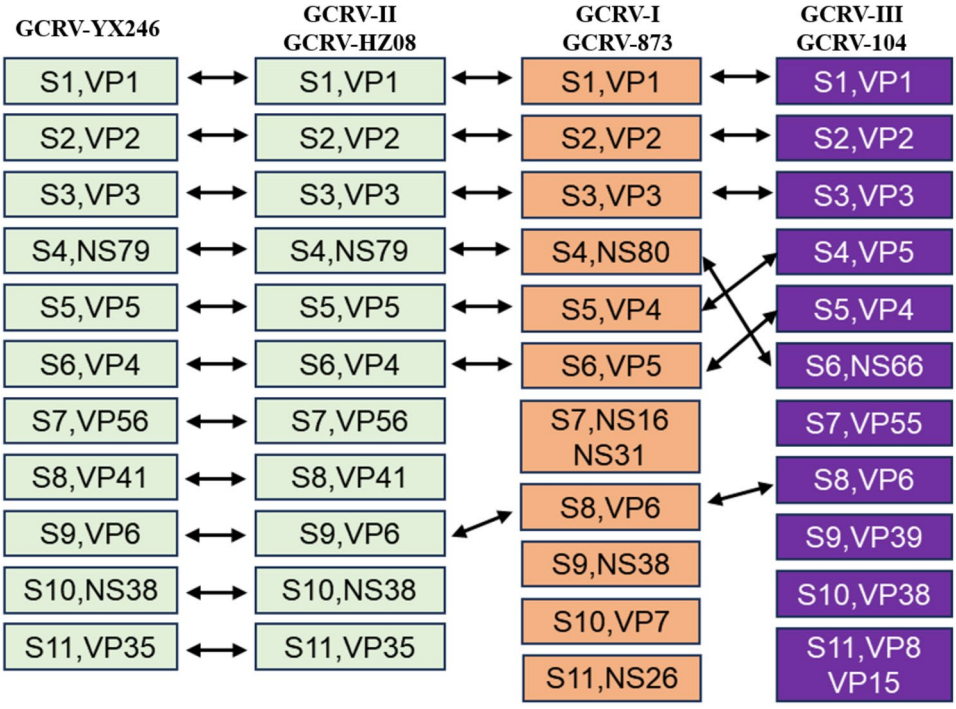

Fig. 4 Sequence analysis of GCRV-YX246. Relationships between predicted proteins in the three GCRV genotypes. Double-headed arrows indicate equivalent proteins across the genotypes

Table 2 Comparison of nucleotide and amino acid sequence identity between GCRV-YX246 and other genotype GCRV strains

segment	GCRV-YX246		GCRV-II		GCRV-I		GCRV-III	
			GCRV-HZ08		GCRV-873		GCRV-104	
	bp	aa	bp(%)	aa(%)	bp(%)	aa(%)	bp(%)	aa(%)
S1	3928	1294	3927 (98.52%)	1294 (98.30%)	3949 (45.49%)	1299 (30.79%)	3943 (44.08%)	1294 (29.72%)
S2	3867	1272	3870 (98.19%)	1273 (98.35%)	3877 (52.90%)	1274 (46.82%)	3864 (51.56%)	1274 (45.82%)
S3	3753	1232	3753 (99.12%)	1232 (99.51%)	3702 (47.42%)	1214 (35.91%)	3729 (48.56%)	1224 (36.76%)
S4	2310	717	2263 (97.37%)	716 (98.53%)	2320 (39.39%)	742 (24.53%)	1912 (40.60%)	609 (32.20%)
S5	2230	726	2229 (96.95%)	726 (98.21%)	2239 (43.56%)	728 (28.49%)	2210 (39.37%)	715 (23.56%)
S6	2028	650	2030 (96.06%)	650 (97.85%)	2039 (44.82%)	648 (33.84%)	2003 (43.13%)	638 (27.11%)
S7	1604	512	1604 (97.26%)	512 (96.68%)	1414 (37.61%)	274/146 (-)	1581 (39.01%)	511 (22.19%)
S8	1560	361	1560 (96.86%)	361 (98.34%)	1296 (39.01%)	412 (-)	1319 (37.27%)	418 (-)
S9	1320	418	1320 (97.12%)	418 (97.85%)	1130 (31.43%)	352 (-)	1141 (39.23%)	354 (-)
S10	1124	345	1124 (98.40%)	345 (99.71%)	909 (38.36%)	276 (-)	1128 (41.43%)	346 (-)
S11	1027	310	1027 (96.79%)	310 (98.39%)	820 (37.81%)	244 (-)	876 (40.69%)	140 (-)
Total genome length Average	24,751	7837	24,707 (98.39%)	7837 (98.35%)	23,695 (42.62%)	7609 (33.44%)	23,706 (42.41%)	7523 (35.85%)

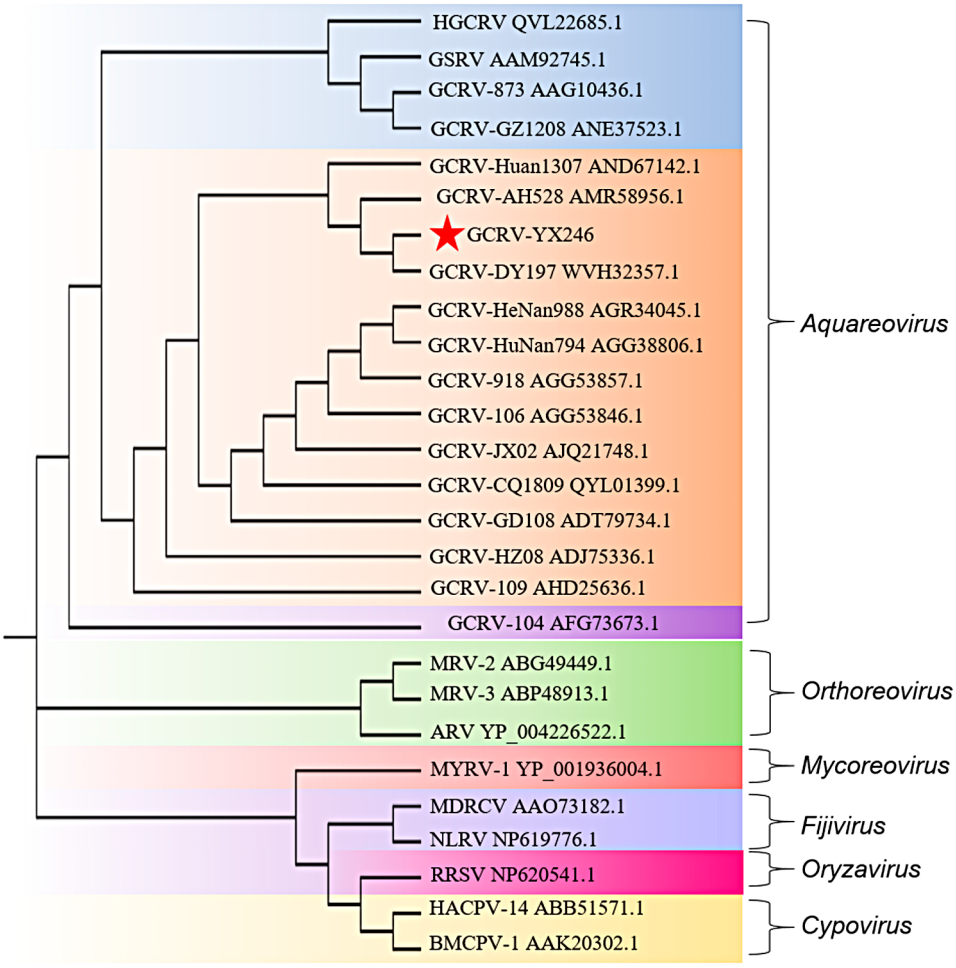

Fig. 5 Phylogenetic relationship of GCRV-YX246 to the *Reoviridae* family. Phylogenetic tree was constructed using the neighbor-joining method with 1,000 bootstrap replicates based on RNA-dependent RNA polymerase (RdRp) amino acid sequences

acid sequence of the highly conserved VP6 protein was constructed. The analysis revealed that grass carp reovirus strains clustered into three genotype groups, with GCRV-YX246 being most closely related to GCRV-AH528 within the GCRV-II group, indicating that GCRV-YX246 likely belongs to the GCRV-II genotype (Fig. 6).

We performed a genomic homology comparison, which further validated the classification of GCRV-YX246 within the GCRV-II clade. Six strains with the highest sequence similarity were selected as reference sequences for this analysis. A phylogenetic tree constructed using the maximum likelihood (ML) method based on whole-genome data indicated that GCRV-YX246 is most closely related to strain GCRV-HN14, though it diverges significantly from the other reference strains (Fig. 7). To investigate whether GCRV-YX246 represents a novel strain, we analyzed the S11 protein sequences across multiple strains. The S11 region in GCRV-YX246 contains a unique protein insertion that may encode an α-helix, distinguishing it from the other six reference strains and reinforcing its classification as a unique strain (Fig. S1). Additionally, we examined evolutionary dynamics by calculating the evolutionary coefficient (πN/πS). The results showed that the πN/πS ratios of all segments decreased following the inclusion of GCRV-YX246, suggesting increased negative selection pressure and indicating that the GCRV sequences have remained relatively stable without undergoing substantial evolutionary changes (Fig. S2). Combined with the differences in clinical pathogenicity, we therefore conclude that this strain should be considered a new strain, distinct from the six previously reported strains.

Artificial infection experiments

To assess the virulence and pathogenicity of GCRV-YX246, healthy rare minnows and grass carp were infected with the virus, and their clinical features, histopathological changes and survival rates were monitored. Infected grass carp and rare minnows exhibited typical hemorrhagic symptoms, including lesions on the gill

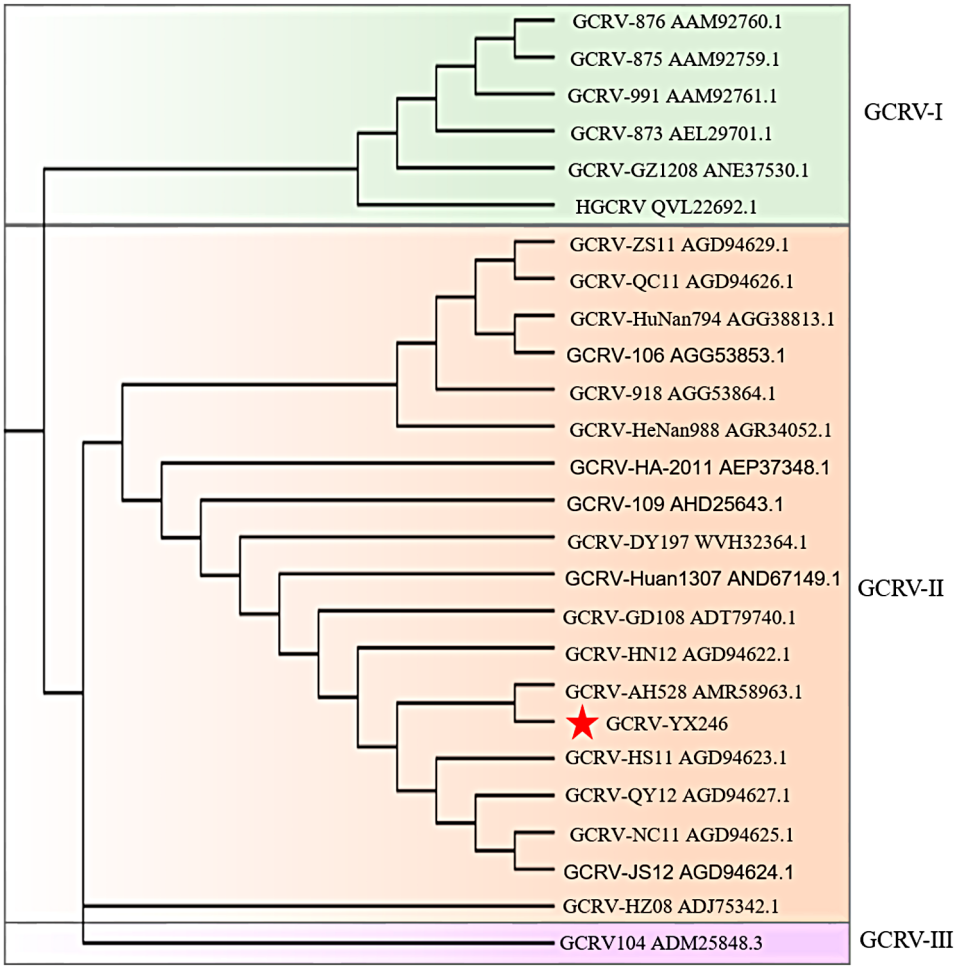

Fig. 6 Phylogenetic analysis of GCRV-YX246 and other GCRV strains was constructed based on the core protein VP6. Phylogenetic tree was performed using the neighbor-joining method with 1,000 bootstrap replicates

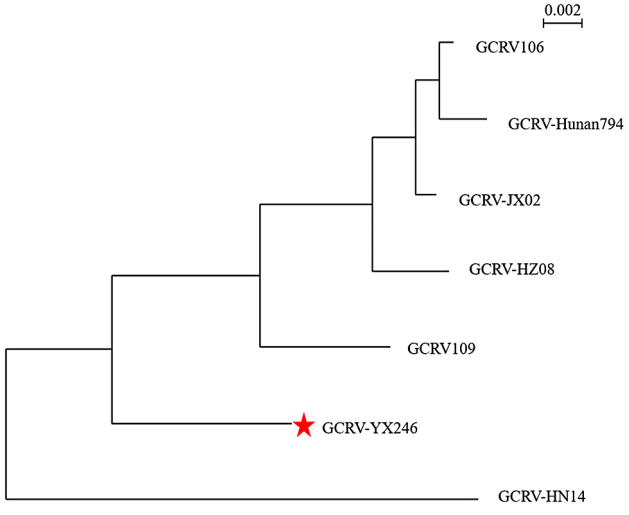

Fig. 7 Phylogenetic analysis of GCRV-YX246 and other GCRV-II strains was conducted using the full genome sequences, and a maximum likelihood (ML) phylogenetic tree was constructed to infer evolutionary relationships

covers, muscles, and mouth, resembling those observed in naturally infected fish (Figs. 8A and 9A). Mortality in both species began at 4 dpi, peaked at 7 dpi, and reached a cumulative rate of over 90% by the end of the 15-day experiment (Figs. 8B and 9B). Postmortem analysis revealed that dead fish harbored significantly higher viral loads in all examined organs (SP, HK, gill, and gut) compared to live infected fish (Figs. 8C and 9C). Immunofluorescence microscopy further confirmed the widespread presence of GCRV in all analyzed organs of infected fish (Figs. 8D and 9D), while GCRV was virtually absent in the organs of control fish (Fig. S3A, 3B). Histological examination revealed that infected fish exhibited necrosis and erythrocyte infiltration in the SP and HK, accompanied by loss of splenic melanomacrophage centers (MMCs). Additionally, significant congestion and extensive tissue damage were observed in the gills and gut compared to control fish (Figs. 8E and 9E).

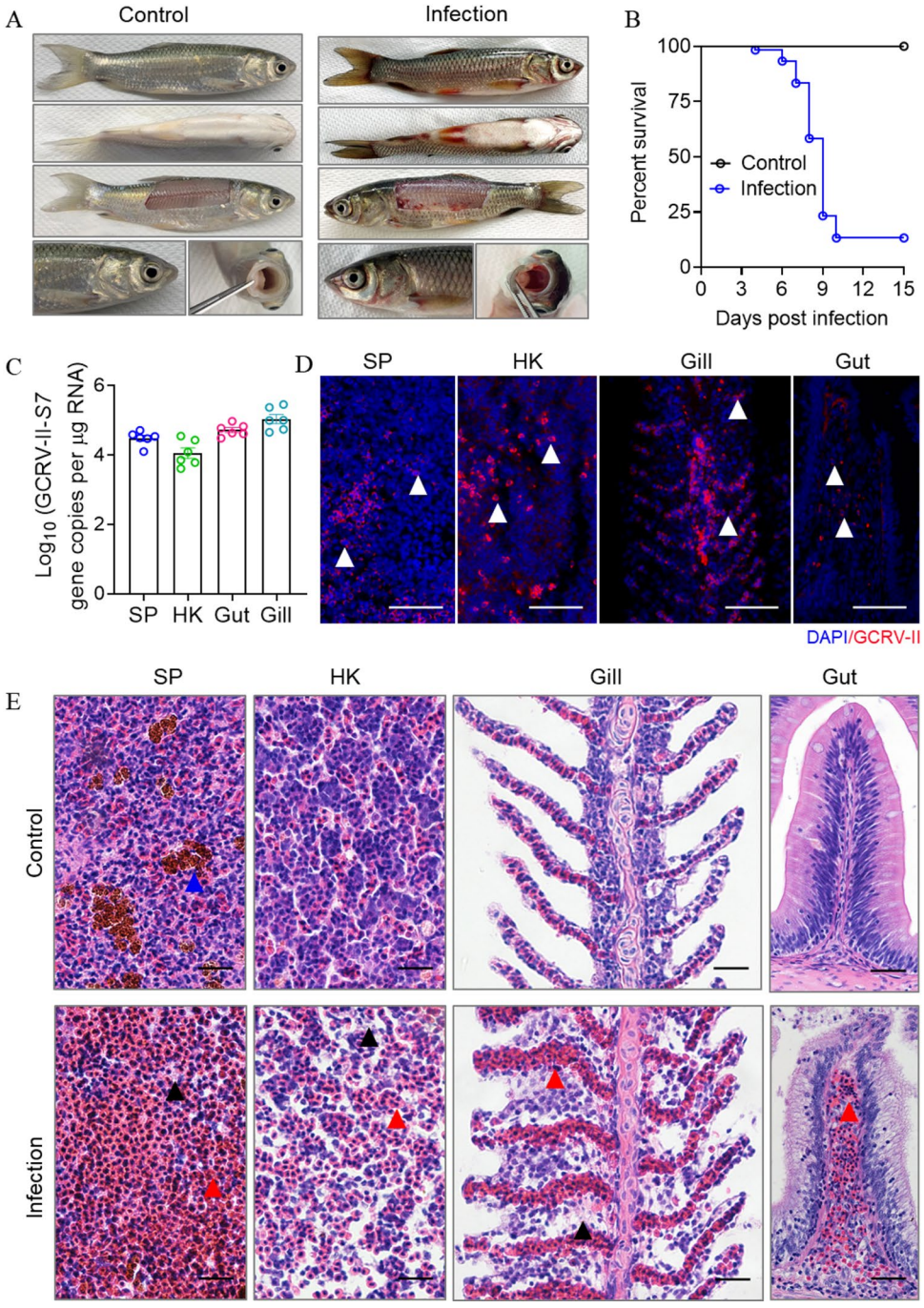

Fig. 8 Pathogenicity analysis of highly pathogenic GCRV-YX246 in grass carp. **A** Hemorrhagic symptoms observed in grass carp 7 days post-infection with GCRV-YX246. **B** Survival curves of grass carp after GCRV-YX246 infection. $n = 60$. **C** Viral loads in various tissues of grass carp post GCRV-YX246 challenge ($n = 6$). The gill and gut exhibited the highest viral loads, followed by the SP and HK. **D** Immunofluorescence assay showing GCRV-II presence in the SP, HK, gut, and gill of infected grass carp (white arrow indicates GCRV-II virus). Scale bar, 50 μm. **E** Histopathological lesions in the SP, HK, gut, and gill of grass carp infected with GCRV-YX246. In the SP, the blue arrows indicate the MMCs, the red arrow shows erythrocyte infiltration, and the black arrows mark cellular necrosis. Scale bar, 50 μm

Discussion

GCHD is among the most severe viral threats to freshwater aquaculture, causing significant economic losses. To date, over 60 strains of GCRV have been isolated, with the virus showing considerable genetic diversity across its three genotypes [14, 22]. Notably, genotype II GCRV has emerged as the predominant strain responsible for GCHD outbreaks in China. Since the 1990s, widespread vaccination has largely controlled the disease, preventing large-scale epidemics, particularly in southern China

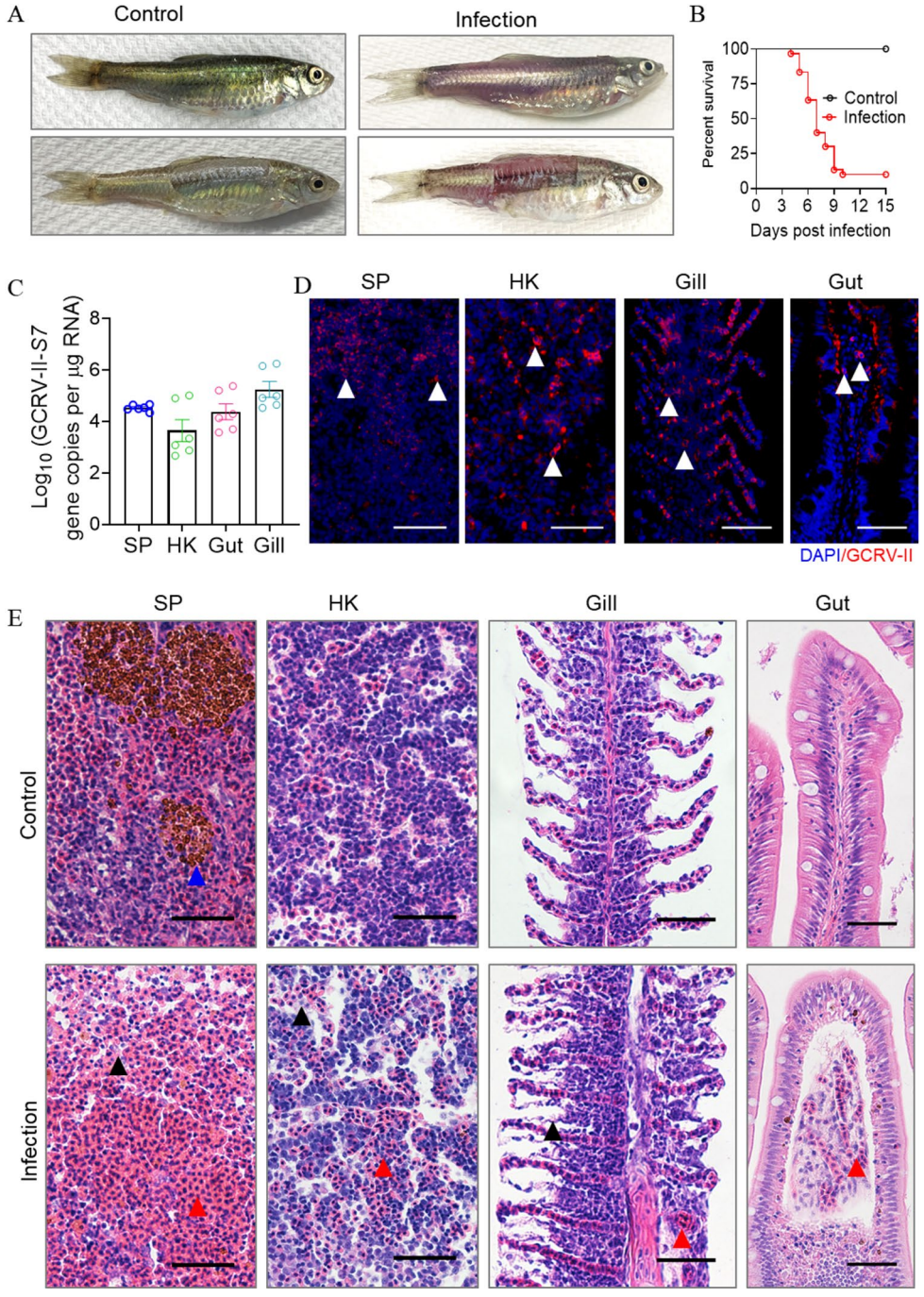

Fig. 9 Pathogenicity analysis of highly pathogenic GCRV-YX246 in rare minnows. **A** Hemorrhagic symptoms observed in rare minnows at 7 days post-infection with GCRV-YX246. **B** Survival curves of rare minnows after GCRV-YX246 infection; $n = 30$. **C** Viral loads in various tissues of rare minnows post GCRV-YX246 challenge ($n = 6$), with the gill and gut exhibiting the highest viral loads, followed by the SP and HK. **D** Immunofluorescence assay demonstrating GCRV-II presence in the SP, HK, gut, and gill of infected rare minnows (white arrow indicates GCRV-II virus). Scale bar, 50 μm. **E** Histopathological lesions in the SP, HK, gut, and gill of rare minnows infected with GCRV-YX246. In the SP, the blue arrow indicate the MMCs, the red arrow shows erythrocyte infiltration, and the black arrows mark cellular necrosis. Scale bar, 50 μm

[23]. However, sporadic outbreaks continue to occur in some fish farms [24]. Around the year 2000, the incidence of GCRV infections began to rise, especially in large grass carp farms situated in the Yangtze and Pearl River basins [25]. This study provides a comprehensive analysis of a GCRV-II infection event in a large grass carp farm in Hubei Province, focusing on genome sequencing and virulence characteristics.

The infected grass carp in this study exhibited classic clinical symptoms of GCHD, including spot- or plate-like

hemorrhages in various tissues, such as the oral cavity, base of the fins, and gill covers, as well as severe petechial hemorrhages in the muscles, intestines, and liver [26]. Based on these symptoms, GCHD can be categorized into three types: red muscle type, enteritis type, and red fin/red gill type [16]. In our study, all infected fish showed signs of these three types, indicating the possibility of a particularly virulent strain. Of particular interest, dying fish were found to have high viral loads in tissues such as the muscle, brain, and skin. Previous studies have also identified the brain as a "virus reservoir" in both natural and latent GCRV-II infections, similar to the neurotropism observed in mammalian reoviruses [27]. While earlier research suggested that the HK was the primary target for GCRV-II invasion [28], our findings suggest that differences in the infection course and viral entry pathways may explain these discrepancies.

Our study further demonstrated that GCRV-II invades both systemic immune tissues (SP and HK) and mucosal tissues (gut and gill), as confirmed by TEM and IF analyses [29]. In the middle and late stages of infection, the virus likely spreads to other tissues via blood circulation [30]. Histopathological examinations of the gut, gill, SP, and HK of naturally infected grass carp revealed distinct pathological changes associated with the high viral loads in these tissues [31]. Notably, the high viral load in gut tissue and the severe damage to gut villi suggest the possibility of GCRV-II entering through oral or gut mucosal routes.

Here, we report the complete genome sequence of GCRV-YX246 and its deduced protein sequences, which show high identity with the homologous proteins of GCRV-II strains. Conserved terminal sequences, 5'-GUAAUUU and 3'-UUCAUC, were identified in all 11 genomic segments of GCRV-YX246 in the non-coding regions (NCRs). Notably, the 3' end sequence "-UCAUC" in GCRV-YX246 is identical to that found in aquareoviruses (AqRVs) and mammalian reoviruses (MRV), while the 5'-GUAAUU sequence is conserved among other GCRV-II isolates, including GCRV-HZ09 and GCRV-109 [32]. When compared to available genome sequences of GCRV-GZ1208 (GCRV-I), GCRV-AH528, GCReV-109 (GCRV-II), and GCRV-104 (GCRV-III), the overall identity of homologous proteins ranged from 23.23 to 99.84%. Specifically, the amino acid identity between GCRV-YX246 and GCRV-AH528, as well as GCReV-109, exceeded 97.66%. Importantly, the S7 segment, which encodes VP56, shows relatively high variation in GCRV-YX246. VP56 is known to have a fibrillar structure and plays a crucial role in viral attachment to host cells during GCRV-II infection [33]. Therefore, S7 may function as a cell attachment protein, influencing viral virulence, tropism, and the spread of GCRV-II. Additionally, GCRV-YX246 does not exhibit significant cytopathic effects (CPE) after incubation in cell cultures. Unlike GCRV-I, which possesses a FAST protein responsible for syncytium formation, GCRV-YX246 lacks this protein. Interestingly [34, 35], while GCRV-II shows strong pathogenicity in fish, it demonstrates weak infectivity at the cellular level, a phenomenon that warrants further investigation into the underlying mechanisms of this differential infection pattern.

Conclusions

In conclusion, we identified a highly virulent strain, GCRV-YX246, infecting large grass carp. By comparing the sequences of various GCRV isolates and conducting genotyping, we have gained insights into the genetic variation and evolution of GCRV. The artificial infection experiment revealed that the GCRV-YX246 was high virulent to grass carp and rare minnow. These findings lay the groundwork for developing GCRV-II vaccines, studying pathogenic mechanisms, and formulating strategies for the prevention and control of GCRV infections.

Abbreviations

GCHD	Grass carp hemorrhagic disease
GCRV	Grass Carp Reovirus
MMCs	Melanomacrophage centers
CPE	Cytopathic effects
AQRVs	Aquareoviruses
ORVs	Orthoreoviruses
H&E	Hematoxylin and eosin
HK	Head kidney
SP	Spleen
qPCR	Quantitative polymerase chain reaction
NCBI	National Center for Biotechnology Information
RdRp	RNA-dependent RNA polymerase
dsRNA	Double-stranded RNA

Supplementary Information

The online version contains supplementary material available at https://doi.org/10.1186/s12985-025-02716-8.

Supplementary Material 1

Acknowledgements

Not applicable.

Author contributions

WGK and ZX conceived the overall project and experimental design. GYD, QSZ, XJY and YS performed most of the experiments, analyzed the data, and contribute to the writing of the original manuscript. LYM, CC, and QQZ contributed to immunofluorescence analysis and morphological detection. ZX conceptualized and supervised the study. All authors read and approved the final manuscript.

Funding

This work was supported by grants from the Agricultural Biological Breeding-2030 Major Project (2023ZD04065) and the National Natural Science Foundation of China (32225050, U24A20461, 32303053).

Data availability

No datasets were generated or analysed during the current study.

Declarations

Ethics approval and consent to participate
All experimental protocols were conducted in accordance with the Guiding Principles for the Keeping and Use of Laboratory Animals and were approved by the Institute of Hydrobiology, Chinese Academy of Sciences (permit number 2023-027).

Consent for publication
Not applicable.

Competing interests
The authors declare no competing interests.

Received: 29 November 2024 / Accepted: 27 March 2025
Published online: 02 April 2025

References

1. Su H, Su JG. Cyprinid viral diseases and vaccine development. Fish Shellfish Immunol. 2018;83:84–95.
2. Yu CC, Wu ML, Jiang YC, Xu XY, Li JL, Shen YB. Transcriptome analysis of the spleen provides insight into the immune regulation of GCRV resistance in grass carp (*Ctenopharyngodon idella*). Mar Biotechnol. 2023;25:557–66.
3. Liu J, Yan YJ, Yan J, Wang JT, Wei J, Xiao J, et al. Multi-omics analysis revealed crucial genes and pathways associated with black carp antiviral innate immunity. Fish Shellfish Immunol. 2020;106:724–32.
4. Wang Q, Zeng WW, Liu C, Zhang C, Wang YY, Shi CB, et al. Complete genome sequence of a reovirus isolated from grass carp, indicating different genotypes of GCRV in China. J Virol. 2012;86(22):12466.
5. Liang XY, Wang Q, Wang HY, Wang XY, Chu PF, Yang C, et al. Grass carp superoxide dismutases exert antioxidant function and inhibit autophagy to promote grass carp reovirus (GCRV) replication. Int J Biol Macromol. 2024;256:128454.
6. Yu XB, Liu GL, Zhu B, Hao K, Ling F, Wang GX. In vitro immunocompetence of two compounds isolated from *Polygala tenuifolia* and development of resistance against grass carp reovirus (GCRV) and *Dactylogyrus intermedius* in respective host. Fish Shellfish Immunol. 2014;41(2):541–8.
7. Wang B, Zhang YB, Liu TK, Shi J, Sun F, Gui JF. Fish Viperin exerts a conserved antiviral function through RLR-triggered IFN signaling pathway. Dev Comp Immunol. 2014;47(1):140–9.
8. Yang C, Su J. Molecular identification and expression analysis of Toll-like receptor 3 in common carp *Cyprinus Carpio*. J Fish Biol. 2010;76(8):1926–39.
9. Chen JM, Chang OQ, Li YY, Wang YY, Liu C, Yin JY, et al. Establishment of a rare minnow (*Gobiocypris rarus*) disease model for grass carp reovirus genotype II. Aquaculture. 2021;533:736133.
10. Chen JM, Li YY, Wang YY, Wu SY, Chang OQ, Yin JY, et al. Establishment of a rare minnow (*Gobiocypris rarus*) model for evaluation of experimental vaccines against a disease induced by grass carp reovirus genotype II. Fish Shellfish Immunol. 2021;117:53–61.
11. He LB, Zhang AD, Pei YY, Chu PF, Li YM, Huang R, et al. Differences in responses of grass carp to different types of grass carp reovirus (GCRV) and the mechanism of hemorrhage revealed by transcriptome sequencing. BMC Genom. 2017;18(1):452.
12. Fan C, Shao L, Fang Q. Characterization of the nonstructural protein NS80 of grass carp reovirus. Arch Virol. 2010;155(11):1755–63.
13. Pei C, Ke F, Chen ZY, Zhang QY. Complete genome sequence and comparative analysis of grass carp reovirus strain 109 (GCReV-109) with other grass carp reovirus strains reveals no significant correlation with regional distribution. Arch Virol. 2014;159(9):2435–40.
14. Ma J, Zeng LB, Fan YD, Zhou Y, Jiang N, Chen Q. Significant Inhibition of two different genotypes of grass carp reovirus in vitro using multiple ShRNAs expression vectors. Virus Res. 2014;189:47–55.
15. Wang Q, Zeng WW, Yin L, Wang YY, Liu C, Li YY, et al. Comparative study on physical-chemical and biological characteristics of grass carp reovirus from different genotypes. J World Aquacult Soc. 2016;47(6):862–72.
16. Mateu MG. Assembly, engineering and applications of virus-based protein nanoparticles. Adv Exp Med Biol. 2016;940:83–120.
17. Liang HR, Fu XZ, Li NQ, Liu LH, Lin Q, Li YG, et al. The distribution of different virulence grass carp reovirus strains in some neglected tissues. Pol J Vet Sci. 2016;19(4):763–70.
18. Lozach PY. Cell biology of viral infections. Cells. 2020;9(11):2431.
19. Moulder JW. Comparative biology of intracellular parasitism. Microbiol Rev. 1985;49(3):298–337.
20. Bøgwald J, Dalmo RA. Protection of teleost fish against infectious diseases through oral administration of vaccines: update 2021. Int J Mol Sci. 2021;22(20):10932.
21. Liu BQ, Zeng WW, Wang Q, Zhang LS, Wang YY, Shi CB, et al. Development of a fluorescent quantitative polymerase chain reaction technique for detection of grass carp reovirus HZ08 strain. J Fish Sci China. 2012;19:329–35.
22. Fang Q, Zhang J, Zhang FX. Molecular Biology of Aquareoviruses, In: Fang, Q, editors. Aquareovirus Springer Singapore. 2021;39–75.
23. Yu CC, Jiang YC, Zhang CY, Wu ML, Gui L, Xu XY, et al. Whole-genome resequencing of grass carp (*Ctenopharyngodon idella*) for genome-wide association study on GCRV resistance. Aquaculture. 2024;592:741243.
24. Mondal H, Thomas J. A review on the recent advances and application of vaccines against fish pathogens in aquaculture. Aquacult Int. 2022;30:1971–2000.
25. Lin S, Milardi M, Gao Y, Wong MH. Sustainable management of non-native grass carp as a protein source, weed-control agent and sport fish. Aquac Res. 2022;53:5809–24.
26. Liang HR, Li YG, Zeng WW, Wang YY, Wang Q, Wu SQ. Pathogenicity and tissue distribution of grass carp reovirus after intraperitoneal administration. Virol J. 2014;11:178.
27. Jiang R, Zhang J, Liao ZW, Zhu WT, Su H, Zhang YG, et al. Temperature-regulated type II grass carp reovirus establishes latent infection in *Ctenopharyngodon Idella* brain. Virol Sin. 2023;38:440–7.
28. Tian QQ, Huo XC, Liu Q, Yang CR, Zhang YG, Su JG. VP4/VP56/VP35 Virus-like particles effectively protect grass carp (*Ctenopharyngodon idella*) against GCRV-II infection. Vaccines. 2023;11:1373.
29. Gao Y, Huo XC, Wang ZS, Yuan GL, Liu XL, Ai TS, et al. Oral administration of *Bacillus subtilis* subunit vaccine significantly enhances the immune protection of grass carp against GCRV-II infection. Viruses. 2021;14:30.
30. Koyuncu OO, Hogue IB, Enquist LW. Virus infections in the nervous system. Cell Host Microbe. 2013;13:379–93.
31. Pandey V, Bhat RAH, Chandra S, Tandel RS, Dubey MK, Sharma P, et al. Clinical signs, lethal dose and histopathological lesions in grass carp, *Ctenopharyngodon Idella* experimentally infected with *Edwardsiella Tarda*. Microb Pathog. 2021;161:105292.
32. Kong WG, Ding GY, Yang P, Li YQ, Cheng GF, Cai C, et al. Comparative transcriptomic analysis revealed potential differential mechanisms of grass carp reovirus pathogenicity. Int J Mol Sci. 2023;24(21):15501.
33. Xu C, Qiao MH, Huo XC, Liao ZW, Su JG. An oral microencapsulated vaccine loaded by sodium alginate effectively enhances protection against GCRV infection in grass carp (*Ctenopharyngodon idella*). Front Immunol. 2022;13:848958.
34. Ciechonska M, Duncan R, Reovirus. FAST proteins: virus-encoded cellular fusogens. Trends Microbiol. 2014;22:715–24.
35. Yan XY, Wang Y, Xiong LF, Jian JC, Wu ZH. Phylogenetic analysis of newly isolated grass carp reovirus. Springerplus. 2014;3:190.

Publisher's note